Stable identification of linear isotropic Cosserat parameters: bounded stiffness in bending and torsion implies conformal invariance of curvature.

Patrizio Neff [*] and Jena Jeong [†] and Andreas Fischle [‡]

February 4, 2009

Abstract

We describe a principle of bounded stiffness and show that bounded stiffness in torsion and bending implies a reduction of the curvature energy in linear isotropic Cosserat models leading to the so called conformal curvature case $\mu \frac{L_c^2}{2} \|\operatorname{dev}\operatorname{sym}\nabla\operatorname{axl}\overline{A}\|^2$ where $\overline{A} \in \mathfrak{so}(3)$ is the Cosserat microrotation. Imposing bounded stiffness greatly facilitates the Cosserat parameter identification and allows a well-posed, stable determination of the one remaining length scale parameter L_c and the Cosserat couple modulus μ_c.

Key words: polar-materials, microstructure, parameter-identification, conformal curvature structured continua, solid mechanics, variational methods.

Contents

[*] Patrizio Neff, Fachbereich Mathematik, Technische Universität Darmstadt, Schlossgartenstrasse 7, 64289 Darmstadt, Germany, email: neff@mathematik.tu-darmstadt.de, Tel.: +49-6151-16-3495 and Chair of Nonlinear Analysis, Fachbereich Mathematik, Universität Duisburg-Essen, Campus Essen, Universitätsstr. 3, 45141 Essen, Germany

[†] Jena Jeong, Ecole Spéciale des Travaux Publics du Bâtiment et de l'Industrie (ESTP), 28 avenue du Président Wilson, 94234 Cachan Cedex, France, email: jeong@profs.estp.fr

[‡] Andreas Fischle, Fachbereich Mathematik, Universität Duisburg-Essen, Campus Essen, Universitätsstr. 3, 45141 Essen, Germany, email: andreas.fischle@uni-due.de

1 Introduction

Non-classical size-effects are becoming increasingly important for materials at the micro- and nanoscale regime. There are many possibilities in order to include size-effects on the continuum scale. One such prominent model is the Cosserat model. In its simplest isotropic linear version the Cosserat model introduces six material parameters. However, the parameter identification for Cosserat solids is a difficult and challenging issue, let us only mention the exhaustive discussion in [4] and references therein.

We show how to a priori reduce the number of curvature parameters in the linear, isotropic, centro-symmetric Cosserat model by requiring what we identify with **bounded stiffness**. First, we recall the Cosserat model and we motivate bounded stiffness in general. Then we apply our result to the torsion and bending of thin circular Cosserat wires. Imposing bounded stiffness reduces the curvature energy to the conformally invariant case which is the weakest possible requirement for well-posedness of the linear isotropic Cosserat model [19].

Our approach here is based on an a priori investigation of given analytical solutions for simple but three-dimensional Cosserat boundary value problems: namely torsion and bending of a circular wire by resultant moments with the understanding that these are the most relevant cases from an experimental point of view.

It is well-known that a Cosserat solid displays size-effects. These size effects refer to a non-classical dependence of rigidity of an object upon one or more of its dimensions. In classical linear elasticity for a circular cylinder with radius a the rigidity in tension is proportional to a^2 and the rigidity in torsion and bending is proportional to a^4. For the Cosserat solid the ratio of rigidity to its classical value is increased: thinner samples of the same material respond stiffer. For certain parameter ranges of the Cosserat solid this effect may be dramatic. For example the rigidity in torsion could become proportional to a^2 such that the normalised torsional rigidity (normalised against the classical value) has a singularity proportional to $\frac{1}{a^2}$. However, as notes already Lakes [23]: "..., infinite stiffening effects are unphysical."

Our principle of bounded stiffness requires simply that the stiffness increase for thinner and thinner samples (normalised against the classical stiffness) should be bounded independent of the wire radius a, i.e. a singularity free response. In bending and torsion we can directly read off the corresponding requirement. It leads in a straight forward way to what we term the conformal curvature case $\mu \frac{L_c^2}{2} \|\operatorname{dev}\operatorname{sym}\nabla\operatorname{axl}\overline{A}\|^2$. In separate contributions [30, 20, 28, 29, 19] we have investigated, in more detail, this novel conformal curvature case from alternative perspectives.

Of the many analytical solutions available in micropolar elasticity [8] we do not consider two-dimensional plane stress or plane strain solutions since the relevance of these boundary value problems hinges on very special isotropy, homogeneity and symmetry assumptions. These solutions, being so special, do only involve one overall curvature parameter. If any singular stiffening behaviour is predicted [14] this would therefore exclude curvature effects altogether.

In this sense this note also corrects some statements towards the same goal of reducing the number of parameters in a linear Cosserat solid made in [27] where, however, plane strain boundary value problems have been included. The conclusions in [27] regarding the consequences of bounded stiffness are therefore corrected and highlighted.

We begin by establishing the linear isotropic Cosserat model [6, 5, 9, 34, 33, 37, 11] along with some of our notation. This section does not contain new results. The remaining notation is found in the appendix.

1.1 The linear elastic Cosserat model in variational form

For the **displacement** $u : \Omega \subset \mathbb{R}^3 \mapsto \mathbb{R}^3$ and the **skew-symmetric infinitesimal microrotation** $\overline{A} : \Omega \subset \mathbb{R}^3 \mapsto \mathfrak{so}(3)$ we consider the **two-field** minimisation problem

$$I(u,\overline{A}) = \int_\Omega W_{\mathrm{mp}}(\overline{\varepsilon}) + W_{\mathrm{curv}}(\nabla\operatorname{axl}\overline{A}) - \langle f, u\rangle \,\mathrm{dV} - \int_{\partial\Omega} \langle f_s, u\rangle - \langle M_s, u\rangle \,\mathrm{dS} \mapsto \quad \min.\ \text{w.r.t.}\ (u,\overline{A})\,, \tag{1.1}$$

under the following constitutive requirements and boundary conditions

$$
\begin{aligned}
\overline{\varepsilon} &= \nabla u - \overline{A}, \quad \textbf{first Cosserat stretch tensor} \\
u_{|_\Gamma} &= u_\mathrm{d}\,, \quad \textbf{essential displacement boundary conditions} \\
W_\mathrm{mp}(\overline{\varepsilon}) &= \mu\,\|\operatorname{sym}\overline{\varepsilon}\|^2 + \mu_c\,\|\operatorname{skew}\overline{\varepsilon}\|^2 + \frac{\lambda}{2}\operatorname{tr}[\operatorname{sym}\overline{\varepsilon}]^2 \qquad \textbf{strain energy} \qquad (1.2)\\
\phi &:= \operatorname{axl}\overline{A} \in \mathbb{R}^3, \quad \overline{\mathfrak{k}} = \nabla\phi\,, \quad \|\operatorname{curl}\phi\|^2_{\mathbb{R}^3} = 4\|\operatorname{axl}\operatorname{skew}\nabla\phi\|^2_{\mathbb{R}^3} = 2\|\operatorname{skew}\nabla\phi\|^2_{\mathbb{M}^{3\times3}} \\
W_\mathrm{curv}(\nabla\phi) &= \frac{\gamma+\beta}{2}\|\operatorname{dev}\operatorname{sym}\nabla\phi\|^2 + \frac{\gamma-\beta}{2}\|\operatorname{skew}\nabla\phi\|^2 + \frac{3\alpha+(\beta+\gamma)}{6}\operatorname{tr}[\nabla\phi]^2\,.
\end{aligned}
$$

Here, f are given volume forces while u_d are Dirichlet boundary conditions for the displacement at $\Gamma \subset \partial\Omega$ where $\Omega \subset \mathbb{R}^3$ denotes a bounded Lipschitz domain. Surface tractions, volume couples and surface couples can be included in the standard way. The strain energy W_mp and the curvature energy W_curv are the most general isotropic quadratic forms in the **infinitesimal non-symmetric first Cosserat strain tensor** $\overline{\varepsilon} = \nabla u - \overline{A}$ and the **micropolar curvature tensor** $\overline{\mathfrak{k}} = \nabla\operatorname{axl}\overline{A} = \nabla\phi$ (curvature-twist tensor). The parameters μ, λ[MPa] are the classical Lamé moduli and α, β, γ are further micropolar curvature moduli with dimension $[\mathrm{Pa}\cdot\mathrm{m}^2] = [\mathrm{N}]$ of a force. The additional parameter $\mu_c \geq 0$[MPa] in the strain energy is the **Cosserat couple modulus**. For $\mu_c = 0$ the two fields of displacement u and microrotations $\overline{A} \in \mathfrak{so}(3)$ decouple and one is left formally with classical linear elasticity for the displacement u.

1.2 The strong form of the linear elastic Cosserat balance equations

The strong form of the Cosserat balance equations are given by

$$
\begin{aligned}
\operatorname{Div}\sigma &= f\,, \qquad \textbf{balance of linear momentum} \\
-\operatorname{Div} m &= 4\,\mu_c\cdot\operatorname{axl}\operatorname{skew}\overline{\varepsilon}\,, \quad \textbf{balance of angular momentum} \qquad (1.3)\\
\sigma &= 2\mu\cdot\operatorname{sym}\overline{\varepsilon} + 2\mu_c\cdot\operatorname{skew}\overline{\varepsilon} + \lambda\cdot\operatorname{tr}[\overline{\varepsilon}]\cdot 1\!\!1 = (\mu+\mu_c)\cdot\overline{\varepsilon} + (\mu-\mu_c)\cdot\overline{\varepsilon}^T + \lambda\cdot\operatorname{tr}[\overline{\varepsilon}]\cdot 1\!\!1 \\
&= 2\mu\cdot\operatorname{dev}\operatorname{sym}\overline{\varepsilon} + 2\mu_c\cdot\operatorname{skew}\overline{\varepsilon} + K\cdot\operatorname{tr}[\overline{\varepsilon}]\cdot 1\!\!1\,, \\
m &= (\gamma+\beta)\operatorname{dev}\operatorname{sym}\nabla\phi + (\gamma-\beta)\operatorname{skew}\nabla\phi + \frac{3\alpha+(\gamma+\beta)}{2}\operatorname{tr}[\nabla\phi]\,1\!\!1\,, \\
\phi &= \operatorname{axl}\overline{A}\,, \quad u_{|_\Gamma} = u_\mathrm{d}\,, \quad m.\vec{n}_{|_{\partial\Omega}} = 0\,.
\end{aligned}
$$

For simplicity we assume here that the microrotations $\overline{A} \in \mathfrak{so}(3)$ remain free at the boundary, thus $m.\vec{n}_{|_{\partial\Omega}} = 0$. This Cosserat model can be considered with basically three different sets of moduli for the curvature energy which in each step relaxes the curvature energy. The situations are characterised by possible estimates for the curvature energy:

1: $W_\mathrm{curv}(\overline{\mathfrak{k}}) \geq c^+\,\|\overline{\mathfrak{k}}\|^2$.

2: $W_\mathrm{curv}(\overline{\mathfrak{k}}) \geq c^+\,\|\operatorname{sym}\overline{\mathfrak{k}}\|^2$.

3: $W_\mathrm{curv}(\overline{\mathfrak{k}}) \geq c^+\,\|\operatorname{dev}\operatorname{sym}\overline{\mathfrak{k}}\|^2$.

The different estimates give rise to to the introduction of representative cases:

1: **pointwise positive case:** $\frac{\mu L_c^2}{2}\|\nabla\phi\|^2$. This corresponds to $\alpha = 0, \quad \beta = 0, \quad \gamma = \mu\,L_c^2$.

2: **symmetric case:** $\frac{\mu L_c^2}{2}\|\operatorname{sym}\nabla\phi\|^2$. This corresponds to $\alpha = 0$, $\beta = \gamma$ and $\gamma = \frac{\mu\,L_c^2}{2}$.

3: **conformal case:** $\frac{\mu L_c^2}{2}\|\operatorname{dev}\operatorname{sym}\nabla\phi\|^2 = \frac{\mu L_c^2}{2}(\|\operatorname{sym}\nabla\phi\|^2 - \frac{1}{3}\operatorname{tr}[\nabla\phi]^2)$. This corresponds to $\beta = \gamma$ and $\gamma = \frac{\mu\,L_c^2}{2}$ and $\alpha = -\frac{1}{3}\mu\,L_c^2$. In terms of the polar ratio $\Psi = \frac{\beta+\gamma}{\alpha+\beta+\gamma}$ it corresponds to the limit value $\Psi = \frac{3}{2}$.

All three cases are mathematically well-posed [19, 27]. The pointwise positive case 1 is usually considered in the literature. Case 2 leads to a symmetric couple-stress tensor m and a new motivation for case 3 is the goal of this investigation. In a plane strain problem all three cases coincide and only one curvature parameter matters, thus not permitting to discern any relation between the three curvature parameters. This is the reason why we exclude plane strain problems.

Case 3 is called the conformal curvature case since the curvature energy is invariant under superposed infinitesimal conformal mappings, i.e. mappings $\phi_C : \mathbb{R}^3 \mapsto \mathbb{R}^3$ that satisfy $\operatorname{dev}\operatorname{sym}\nabla\phi_C = 0$. Such mappings infinitesimally preserve shapes and angles [28]. In that case, the couple stress tensor m is symmetric and trace free. In case 2 and case 3 the constitutive couple stress/curvature tensor relation cannot be inverted.

2 Restrictions imposed by bounded stiffness

We turn now our attention to the practical aspects of the problem of determining material parameters. We investigate the question for which parameter values $(\mu_c, \alpha, \beta, \gamma)$ the linear elastic Cosserat model can be considered to be a consistent description for a continuous solid showing size-effects. We assume the continuous solid to be available in any small size we can think of (this possibility is certainly included in the very definition of a continuous solid). Note that this assumption **excludes** e.g. man made grid-structures but includes e.g. polycrystalline material. We are investigating the situation when one or several dimensions of the specimen get small. Denoting by a such a dimension, the limit $a \to 0$ is purely formal in the sense that we are only interested in the leading order behaviour for small, but not arbitrarily small a. Understanding this limiting process $a \to 0$ opens us, indirectly, the possibility to bound the stiffness of the material at smallest reasonable specimen size away from unrealistic orders of magnitude. For our investigation we study simple three-dimensional boundary value problems for which analytical solutions are available.

2.1 The torsion problem

In a thought experiment we subject the hypothetical continuous solid first to torsion for every slenderness we choose. In [13, 12] the analytical solution for pure torsion of a circular cylinder with radius $a > 0$ and length $L > 0$ is developed under the assumption of translational symmetry in axial direction (the classical solution is equally axisymmetric). For our purpose it is sufficient to look at the **non-dimensional** quantity $\boldsymbol{\Omega}_{\mathrm{t}}$, which compares the classical response with the corresponding micropolar result.

The classical relation between **torque** $Q\,[\mathrm{N}\cdot\mathrm{m}]$ and **twist per unit length** $\frac{\theta}{L}\,[1/\mathrm{m}]$ is given by

$$Q = \mu\, J\, \boldsymbol{\Omega}_{\mathrm{t}} \cdot \frac{\theta}{L}\,, \quad \boldsymbol{\Omega}_{\mathrm{t}} \equiv 1\,, \tag{2.1}$$

where $\mu > 0$ is the **classical shear modulus** coinciding with the corresponding Lamé constant while $J = \frac{\pi\, a^4}{2}$ is the polar moment of inertia of the circular cross section.

Performing the appropriate non-dimensionalization, it can be seen that in any theory without size-effects one has [10]

$$\frac{Q}{a^3}\,[\mathrm{MPa}] = h\left(\frac{\theta}{L}\, a\right)\,, \quad \xi := \frac{\theta}{L}\, a\,, \tag{2.2}$$

where $h : \mathbb{R} \to \mathbb{R}$ is a function $h(\xi)$ that has no other explicit dependence on the wire radius $a > 0$. $\frac{Q}{a^3}$ is a stress-like normalised torque and $\xi := \frac{\theta}{L}\, a$ is the non-dimensional shear at the outer radius. In the linear case one has $h(\xi) = \mu\, \frac{\pi}{2}\, \xi$.

In any experiment with size-effects, the response function h will display this size effect by explicitly depending also on the radius $a > 0$ and we expect that for smaller radius a the larger $h(a, \xi)$ as a function of ξ with $h(a, 0) = 0$, $a \geq 0$. This increase of stiffness for the response function is a commonplace observation for many materials at small length-scales. Here, the stiffness of the material is defined as the slope of h at given $a \geq 0$ for $\xi = 0$ i.e.

$$\text{stiffness} = \left[\partial_\xi h(a, \xi)\right]_{|\xi=0}\,. \tag{2.3}$$

Hence, in general, the stiffness is also a function of the radius a. In the classical linear elastic case $\partial_\xi h(a, \xi)_{|\xi=0} = \mu\, \frac{\pi}{2}$ is independent of the wire radius a. We expect also that stiffness increases for smaller $a > 0$, i.e. $\left[\partial_\xi h(a_2, \xi)\right]_{|\xi=0} \geq \left[\partial_\xi h(a_1, \xi)\right]_{|\xi=0}$ for $a_2 \leq a_1$. However, for any small wire radius $a > 0$ which we investigate, we expect **bounded stiffness** since the

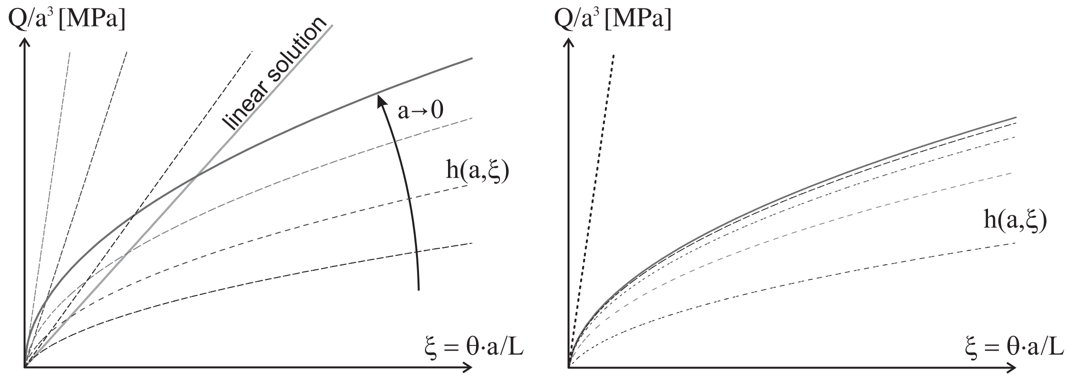

Figure 1: Idealised response curves with size-effects in torsion. Normalised torque $\frac{Q}{a^3}$ versus non-dimensional shear $\xi = \frac{\theta}{L}\,a$ at the outer radius. In general, as $a > 0$ gets smaller, the response gets stiffer. Left: response curves with unbounded stiffness (tangent) as $a \to 0$. Bounded stiffness implies that the left picture is unphysical. Right: stiffness increase with bounded stiffness as $a \to 0$. For linear models, only tangents in 0 are relevant.

constitutive substructure is never completely rigid. This means that there exists a constant K^+ such that

$$\sup_{a\geq 0}\,[\partial_\xi h(a,\xi)]_{|\xi=0} \leq K^+\,. \tag{2.4}$$

2.1.1 The micropolar torsion solution

Now we turn to the linear micropolar model with size-effects (1.3) and consider the generated stiffness depending on the radius a. Since the model is linear, we need only to look at the corresponding factor $\mathbf{\Omega}_{\rm t}$ in (2.1). For the analytical torsion solution in the linear micropolar case it is the assumed that the macroscopic resultant net torque is the sum of the torque due to classical torques (the classical part) $Q_{\rm class}$ and the contribution of the micropolar couples $Q_{\rm cp}$ at the end surface of the wire [15, 18]. On this basis according to [13, 12, 2] it holds in the linear micropolar case[1]

$$\begin{aligned}
Q &= Q_{\rm class} + Q_{\rm cp} = \int_{\partial\Omega^+} (x\,\sigma_{32} - y\,\sigma_{31}) + m_{33}\;{\rm dx\,dy} = \mu\; J\; \mathbf{\Omega}_{\rm t}\;\cdot\frac{\theta}{L}\,,\\
\mathbf{\Omega}_{\rm t} &= 1 + 6\left(\frac{\ell_t}{a}\right)^2\cdot\left(\frac{1-\frac{4}{3}\Psi\cdot\mathcal{X}(p\,a)}{1-\Psi\cdot\mathcal{X}(p\,a)}\right)\,,
\end{aligned} \tag{2.5}$$

where $\partial\Omega^+$ is the top surface of the cylindrical wire and

$$\begin{aligned}
\Psi &:= \frac{\beta+\gamma}{\alpha+\beta+\gamma}\,, \qquad \text{non-dimensional polar ratio}\,, \quad 0\leq\Psi\leq\frac{3}{2}\,,\\
\ell_t^2 &:= \frac{\beta+\gamma}{2}\frac{1}{\mu}\,, \qquad \text{"characteristic length for torsion"}\,,\\
\mathcal{X}(\xi) &:= \frac{I_1(\xi)}{\xi\;I_0(\xi)}\,, \qquad p^2 := \frac{4\,\mu_c}{\alpha+\beta+\gamma} = \frac{2\,\mu_c\,\Psi}{\mu\,\ell_t^2}\,,\\
&I_1(\xi),\,I_0(\xi)\,, \qquad \text{modified } \textbf{Bessel functions} \text{ of the first kind}\,.
\end{aligned} \tag{2.6}$$

Whether or not the model shows bounded stiffness depends solely on the factor $\mathbf{\Omega}_{\rm t}$ in (2.5). In [27] it is shown that $\mathcal{X}(\xi) \sim \frac{1}{2}(1-\frac{\xi^2}{8})$ for small ξ. Therefore, for small radius a the leading

[1] In order to avoid misinterpretations: the analytical torsion solution is based on the assumption of axi-symmetry around the e_3-axis (variables r, θ, z), pure torsion without warping and that the stress tensor σ and couple-stress tensor m are independent of height z. This excludes that $m_{33} = 0$ at the top and bottom of the circular wire. Therefore, microrotations $\overline{A}$ are not free at the extremities and as a result m_{33} is non-zero constant over the height. It seems to be the reason why $\mu_c \to 0$ does not imply that $\mathbf{\Omega}_{\rm t} \to 1$. A generalisation of the solution to arbitrary cross-section has been given in [35] and in [18] the case of anisotropic and inhomogeneous Cosserat coefficients has been treated.

order behaviour of $\mathbf{\Omega}_{\rm t}$ is

$$\mathbf{\Omega}_{\rm t} = 1 + 6\left(\frac{\ell_t}{a}\right)^2\left(\frac{1-\frac{2}{3}\Psi+\frac{4}{3}\Psi\,\frac{p^2a^2}{8}}{1-\frac{\Psi}{2}+\frac{\Psi}{16}p^2a^2}\right) = 1 + 6\left(\frac{\ell_t}{a}\right)^2\left(\frac{1-\frac{2}{3}\Psi+\frac{\Psi^2}{6}\frac{\mu_c}{\mu}\left(\frac{a}{\ell_t}\right)^2}{1-\frac{\Psi}{2}+\frac{\Psi^2}{8}\frac{\mu_c}{\mu}\left(\frac{a}{\ell_t}\right)^2}\right). \tag{2.7}$$

This expression captures the leading order response if $p^2\,a^2 \ll 1$ or $\frac{2\mu_c\,\Psi}{\mu}\left(\frac{a}{\ell_t}\right)^2 \ll 1$.[2] Note that $\mathbf{\Omega}_{\rm t}(a,\ell_t)$ is a continuous function at $(0,0)$ for $\Psi = \frac{3}{2}$ but discontinuous at $a = 0$ for $0 \le \Psi < \frac{3}{2}$.

2.1.2 The response under pure torsion for small radius $a \to 0$

We are interested in what happens to the factor $\mathbf{\Omega}_{\rm t}$ in (2.5), if we let formally $a \to 0$. As we have seen, from a physical point of view the stiffness for smaller radius should be larger than the classical one but the stiffness should certainly remain bounded since the heterogeneity of the microstructure of the physical body can never be perfectly rigid.

For $\mathbf{\Omega}_{\rm t}$ to remain bounded for $\ell_t > 0$ as $a \to 0$ it is **necessary and sufficient** that for small $a > 0$ there exists a constant K^+, independent of a such that

$$\left(\frac{1-\frac{4}{3}\Psi\mathcal{X}(p\,a)}{1-\Psi\,\mathcal{X}(p\,a)}\right) \sim K^+\,a^2 \;\Leftrightarrow$$

$$\lim_{a\to 0}\left(\frac{1-\frac{4}{3}\Psi\mathcal{X}(p\,a)}{1-\Psi\,\mathcal{X}(p\,a)}\right) = \frac{1-\frac{4}{3}\Psi\frac{1}{2}}{1-\Psi\,\frac{1}{2}} = 0 \;\Leftrightarrow\; \Psi = \frac{3}{2}\,. \tag{2.8}$$

Bounded stiffness in torsion and the possibility to describe size-effects within the linear Cosserat model is, therefore, only possible by taking the value $\Psi = \frac{3}{2}$.[3] We visualise the normalised (with respect to the classical size independent rigidity) torsional rigidity $\mathbf{\Omega}_{\rm t}$ versus radius $a > 0$ in the Figure 2 and Figure 3.

In the case $\Psi = \frac{3}{2}$ we have as leading term for $\frac{a}{\ell_t} \ll 1$

$$\mathbf{\Omega}_{{\rm t}|_{a=0}} = 1 + 9\,\frac{\mu_c}{\mu}\,, \qquad \mu_c = \mu\,\frac{\mathbf{\Omega}_{{\rm t}|_{a=0}} - 1}{9}\,, \tag{2.9}$$

which allows us to read off immediately the value for μ_c given the maximally observed stiffness increase in experiment. This formula also shows that μ_c in this interpretation will be independent of the torsional length scale ℓ_t.

In order to understand better the singular behaviour of $\mathbf{\Omega}_{\rm t}$ let us abbreviate (the slope) $s = \frac{\ell_t}{a}$. Then

$$\mathbf{\Omega}_{\rm t}(s) = 1 + 6\,s^2\cdot\left(\frac{1-\frac{4}{3}\Psi\cdot\mathcal{X}(\sqrt{\frac{2\mu_c\,\Psi}{\mu}}\,\frac{1}{s})}{1-\Psi\cdot\mathcal{X}(\sqrt{\frac{2\mu_c\,\Psi}{\mu}}\,\frac{1}{s})}\right). \tag{2.10}$$

For $s \to \infty\,(a \to 0)$ we obtain to leading order

$$\mathbf{\Omega}_{\rm t}(s)_{|_{\Psi<\frac{3}{2}}} \sim 1 + 6\,s^2\,\frac{1-\frac{2}{3}\Psi+\frac{\Psi^2}{6}\frac{\mu_c}{\mu}\frac{1}{s^2}}{1-\frac{\Psi}{2}+\frac{\Psi^2}{8}\frac{\mu_c}{\mu}\frac{1}{s^2}}\,, \qquad \mathbf{\Omega}_{\rm t}(s)_{|_{\Psi=\frac{3}{2}}} \sim 1 + \frac{9\,\frac{\mu_c}{\mu}}{1+\frac{9}{8}\frac{\mu_c}{\mu}\frac{1}{s^2}}\,, \tag{2.11}$$

while for $s \to 0\,(\ell_t \to 0)$ we get

$$\mathbf{\Omega}_{\rm t}(s) \sim 1 + 6\,s^2\,, \tag{2.12}$$

where we have used that $\mathcal{X}(\xi) \to 0$ as $\xi \to \infty$.

In Figure 6 the sensitivity of a determination of Ψ from a torsion experiment is shown.

[2] Taking the limit $\mu_c \to \infty$ in this formula is therefore not possible.

[3] Also foams and bones are not a continuous solid and the argument regarding thinner and thinner samples does therefore not strictly apply, in [22, 24] the value $\Psi = \frac{3}{2}$ has been chosen in order to accommodate bounded stiffness with experimental findings. For a syntactic foam [22, 23] $\beta = \gamma$ has been taken for a best fit. In this case, the curvature energy looks like $W_{\rm curv}(\nabla\phi) = \gamma\,\|\,\mathrm{dev\,sym}\,\nabla\phi\|^2$ with $\gamma > 0$. This is also the best fit for human bone [23, Table 1] and [40]. However, for a polyurethane foam [22] $\beta \neq \gamma$ has been identified and the curvature energy looks like $W_{\rm curv}(\nabla\phi) = \frac{\beta+\gamma}{2}\,\|\,\mathrm{dev\,sym}\,\nabla\phi\|^2 + \frac{\gamma-\beta}{4}\,\|\,\mathrm{curl}\,\phi\|^2$. These examples show on the one hand the relevance of the conformal case and on the other hand that Lakes himself did not formulate a "principle" of bounded stiffness.

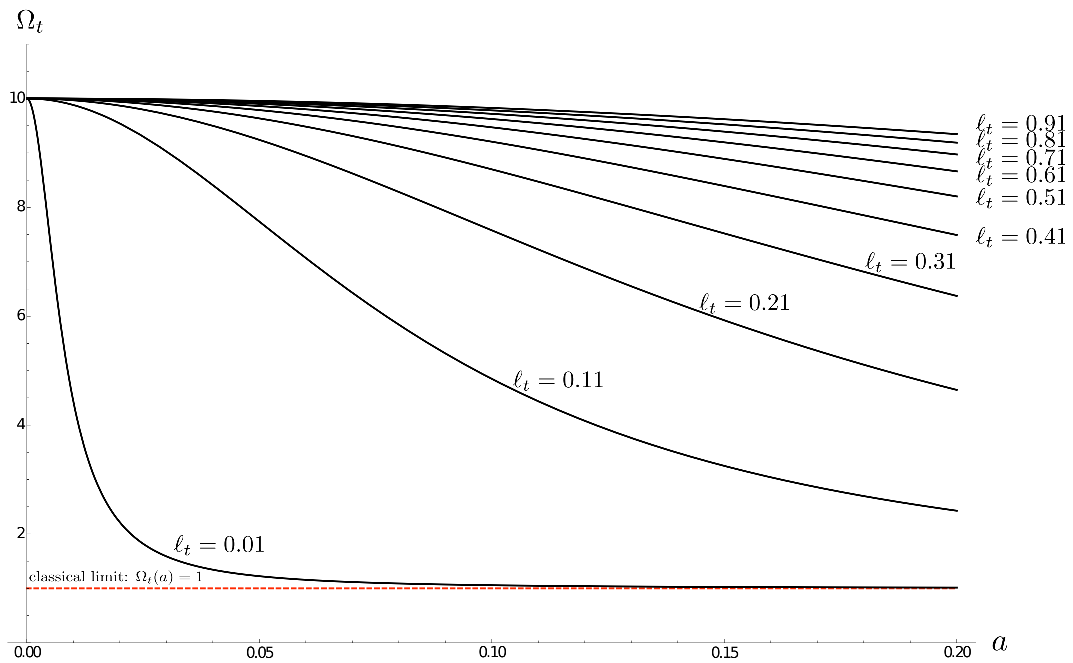

Figure 2: Bounded normalised stiffness in torsion. Plot of $\mathbf{\Omega}_{\rm t}$ versus wire radius a for $\mu_c/\mu = 1$ and polar ratio $\Psi = \frac{3}{2}$. Maximal increase of $\mathbf{\Omega}_{\rm t}$ (vertical axis) for small radius a, i.e. $\mathbf{\Omega}_{{\rm t}|_{a=0}}$ determines uniquely μ_c owing to equation (2.9). We observe a singularity free response and the size of ℓ_t is determined by the range where size effects appear.

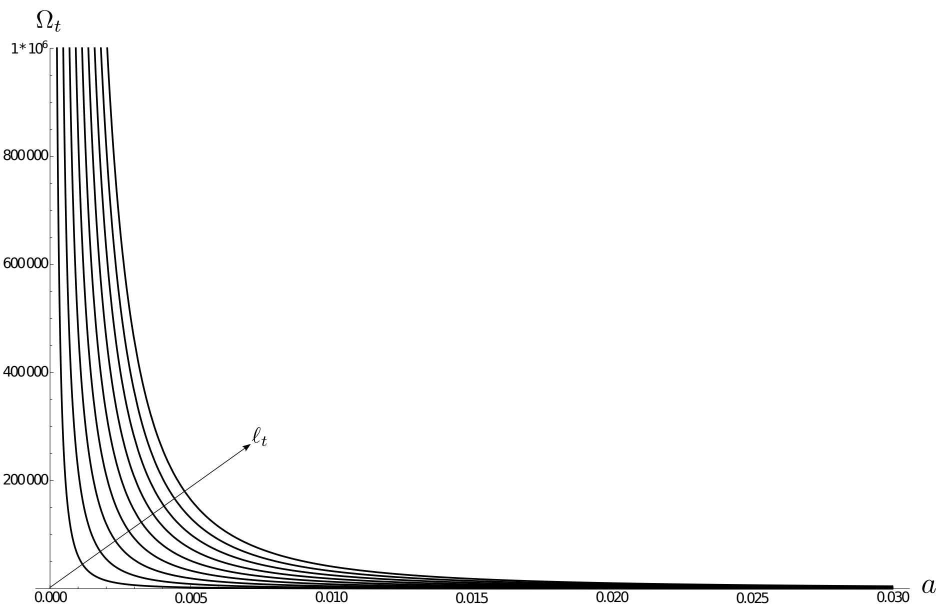

Figure 3: Singular normalised stiffness in torsion. Plot of $\mathbf{\Omega}_{\rm t}$ versus wire radius a for $\mu_c/\mu = 1$ and polar ratio $\Psi = \frac{2}{3}$ ($\alpha = \beta = \gamma$). Unbounded increase of $\mathbf{\Omega}_{\rm t}$ (vertical axis) for small radius a, i.e. $\lim_{a\to 0} \mathbf{\Omega}_{{\rm t}|_a} = \infty$. For a smallest experimentally investigated specimen with radius a_0 the region $(0, a_0]$ of the stiffness response is usually ignored: this corresponds to the folklore that in a Cosserat model the specimen size may not be arbitrary small. Highly sensitive dependency of μ_c and ℓ_t with respect to the cut-off length (smallest investigated wire radius a_0).

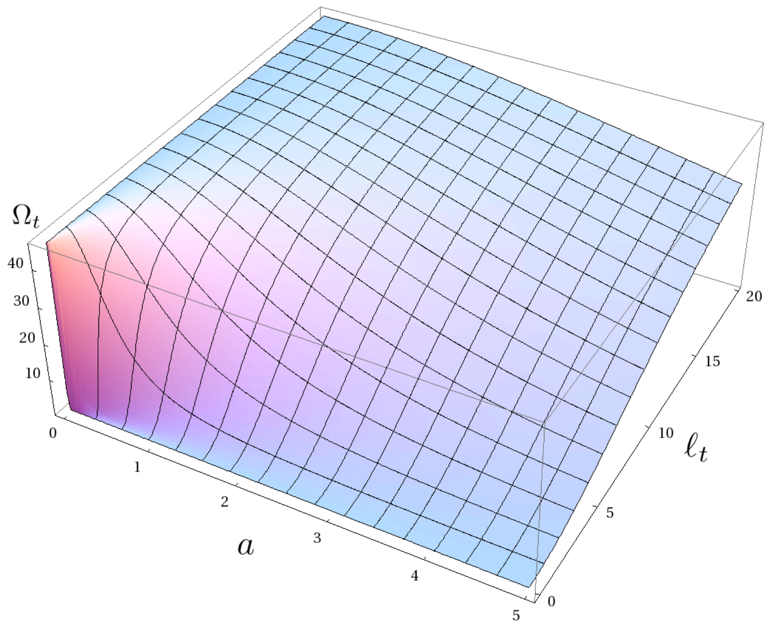

Figure 4: Bounded normalised stiffness in torsion. Plot of $\mathbf{\Omega}_\mathrm{t}$ versus wire radius a and length scale ℓ_t for $\mu_c/\mu = 5$ and polar ratio $\Psi = \frac{3}{2}$. Here, $\mathbf{\Omega}_\mathrm{t}$ is a continuous function, increasing for increasing ℓ_t if $a > 0$ and assuming the constant value $\mathbf{\Omega}_\mathrm{t} = 1 + 9\,\frac{\mu_c}{\mu}$ for $a = 0$ which is independent of ℓ_t, allowing to obtain a size-independent, stable identification of μ_c.

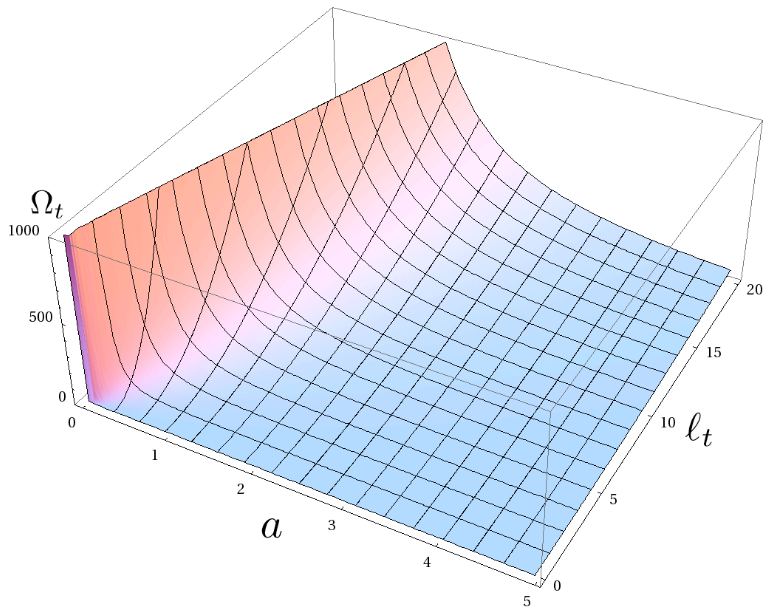

Figure 5: Singular normalised stiffness in torsion. Plot of $\mathbf{\Omega}_\mathrm{t}$ versus wire radius a and length scale ℓ_t for $\mu_c/\mu = 5$ and polar ratio $\Psi = \frac{2}{3}$ $(\alpha = \beta = \gamma)$. $\mathbf{\Omega}_\mathrm{t}$ is discontinuous at $a = 0$ and there is no possibility to influence the behaviour near $a = 0$ by varying μ_c/μ, see (2.11).

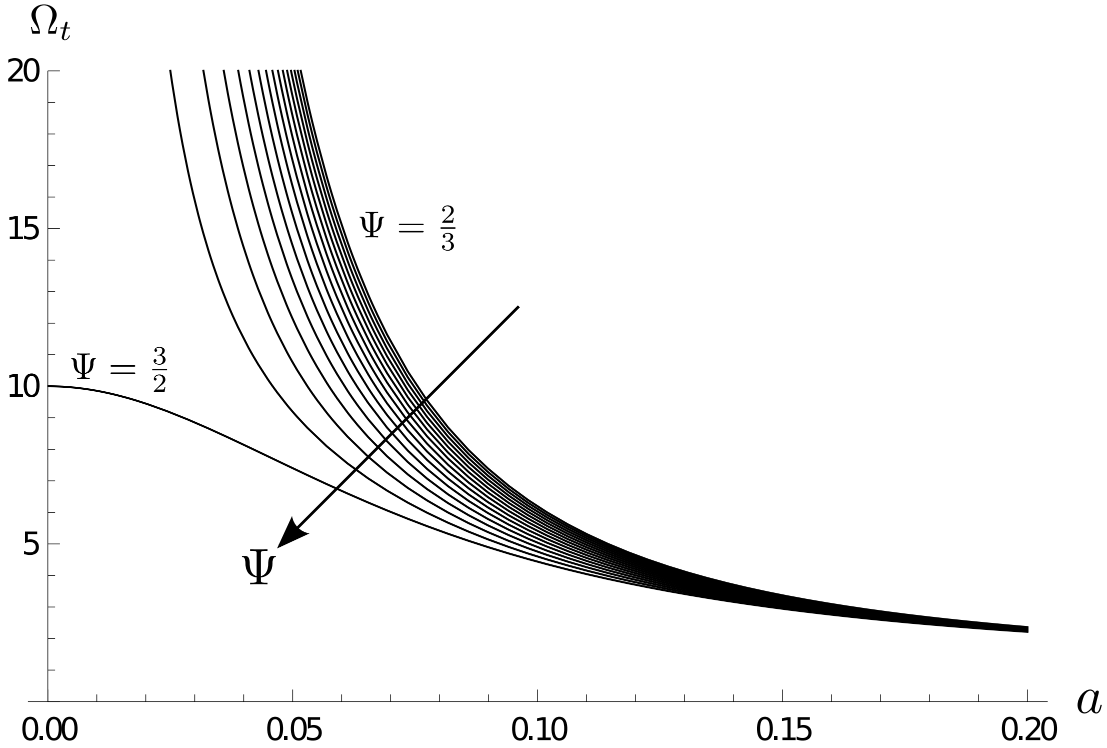

Figure 6: Variation of $\mathbf{\Omega}_{\rm t}$ versus a at $\ell_t = 0.1$ and $\mu_c/\mu = 1$ for different polar ratio $\Psi \in [\frac{2}{3}, \frac{3}{2}]$. This is, in fact, a variation of α alone. The limit $\Psi \to \frac{3}{2}$ is singular.

2.2 The pure bending problem of a cylinder with circular cross-section

2.2.1 The analytical solution

An analytical solution formula for the bending of a micropolar circular cylinder under opposite compressive axial loads with radius $a > 0$ and length $L > 0$ has been obtained in [36]. Similarly as in the torsion case, we focus on the relative stiffness factor $\mathbf{\Omega}_{\rm b}$ compared to classical elasticity. According to [36, 17] it holds that

$$\begin{aligned}
\mathbf{\Omega}_{\rm b} &= 1 + \frac{8\,N^2}{\nu+1}\left(\frac{1-\left(\frac{\beta}{\gamma}\right)^2}{(\delta\,a)^2} + \frac{\left(\left(\frac{\beta}{\gamma}\right)+\nu\right)^2}{\zeta(\delta\,a) + 8\,N^2\,(1-\nu)}\right)\,,\\
\zeta(\xi) &= \xi^2\,\frac{\xi\,I_0(\xi) - I_1(\xi)}{\xi\,I_0(\xi) - 2\,I_1(\xi)}\,, \qquad \delta^2 = \frac{4\,\mu_c\,\mu}{\gamma\,(\mu+\mu_c)} = \frac{4\,N^2\,\mu}{\gamma} = \frac{N^2}{\ell_b^2}\,,\\
\ell_b^2 &= \frac{\gamma}{4\mu}\,, \qquad \text{"characteristic length for bending"}\,, \qquad\qquad (2.13)\\
N^2 &:= \frac{\mu_c}{\mu+\mu_c}\,, \qquad \text{Cosserat coupling number}, \quad 0 \le N \le 1\,,
\end{aligned}$$

and $\nu = \frac{\lambda}{2\,(\mu+\lambda)}$ the classical Poisson ratio. Note that in this setting, the bending moments are applied such that microrotations do not remain free at the surface where these moments are applied. Note that the bending solution does not involve the polar ratio Ψ and therefore includes no information on the curvature parameter α.

2.2.2 The response under pure bending for small wire radius $a \to 0$

For positive Cosserat couple modulus $\mu_c > 0$ and non-vanishing bending length scale $\ell_b > 0$ we are interested in the behaviour of $\mathbf{\Omega}_{\rm b}$ as $a \to 0$. For small $a > 0$ the first term in the bracket of $\mathbf{\Omega}_{\rm b}$ dominates and for $\mathbf{\Omega}_{\rm b}$ to remain bounded as $a \to 0$ (and $\gamma > 0$) one must have

$$(\gamma+\beta)\,(\gamma-\beta) \le 0\,. \qquad (2.14)$$

Since both factors must be positive anyway (1.2) it follows that either $(\gamma+\beta) = 0$ or $(\gamma-\beta) = 0$. In this last case, the Cosserat model still shows size effects in bending (provided $\gamma > 0$) and bounded stiffness.

3 Bounded stiffness implies conformal curvature

Gathering the results implied by the stipulation of bounded stiffness for $0 < \mu_c < \infty$ and arbitrary slender samples we have

1. torsion of a cylinder: $\beta + \gamma = 0$ or $\Psi = \frac{\beta+\gamma}{\alpha+\beta+\gamma} = \frac{3}{2}$.
2. bending of a cylinder: $(\beta + \gamma)(\gamma - \beta) = 0$.

Taking $\beta + \gamma = 0$ is impossible because size-effects would be cancelled altogether. The only consistent choice with these conditions showing on the one hand size-effects at all and bounded stiffness in torsion and bending is therefore $\beta = \gamma = \mu \frac{L_c^2}{2}$ and $\Psi = \frac{3}{2}$. This implies that the curvature energy of the linear isotropic Cosserat solid must look like

$$\mu \frac{L_c^2}{2} \|\operatorname{dev}\operatorname{sym}\nabla\operatorname{axl}\overline{A}\|^2 , \tag{3.1}$$

which is nothing else than the conformal curvature case 3. In terms of the characteristic length for torsion and bending the conformal case is equivalent to

$$\Psi = \frac{3}{2} , \quad \ell_t = 2\,\ell_b . \tag{3.2}$$

Despite the non-invertibility of the corresponding couple stress tensor/curvature tensor relation this problem is amenable to a consistent numerical treatment [20]. In case of the indeterminate couple stress model [16, 1, 25, 38, 21] which appears through the identification $\operatorname{axl}\overline{A} = \frac{1}{2}\operatorname{curl} u$ (formally $\mu_c \to \infty$ or $N \to 1$) the requirement of bounded stiffness in bending (see also [3, eq.60], $\eta = 1$ therein) leads to a symmetric curvature term $\|\operatorname{sym}\nabla\operatorname{curl} u\|^2$, while it is impossible to satisfy bounded stiffness in torsion! Note that a symmetric curvature expression has also been motivated in [39] and applied in [32]. The symmetric curvature expression formally violates uniform positivity of the curvature energy but the model is nevertheless well-posed. Moreover, we can still say that the indeterminate couple stress model with symmetric curvature is conformally invariant [28].

3.1 The classical limit $\mu_c \to 0$ for conformal curvature

In principle, we expect the stiffness factors $\mathbf{\Omega}_{\mathrm{t}}, \mathbf{\Omega}_{\mathrm{b}}$ to approach their classical limit if we let $\mu_c \to 0$ at positive length-scales $\ell_t, \ell_b > 0$. This is automatically true if microrotations remain unconstrained at the boundary. However, for our torsion and bending solutions this is only true if we choose $\Psi = \frac{3}{2}$ and $\beta^2 = \gamma^2$ as is shown in [27]. The reason for this is that the boundary conditions used in the derivation of the analytical formula involve implicit constraints on the microrotations at the top and bottom surface of the circular wire where torsion is applied.

4 Insensitive conformal parameter identification

Regarding parameter identification of hierarchical materials we can offer also another interpretation of bounded stiffness. Bounded stiffness amounts to the requirement that the material is Cauchy elastic on all individual structural levels of investigation. The size-effect is therefore entirely due to geometrical features of the material. Let us explain this statement:

Regarding Figure 3 shows that in the presence of a singularity for smaller radius a the inverse problem of determining the length scale L_c depends sensitively on the thinnest experimentally investigated sample: the slope increases without bounds for small a and the determination of the polar ratio Ψ is extremely sensitive because it requires very thin specimens in general.

In the conformal case this sensitivity is circumvented: one may probe the smallest structural element (or even assume that it is Cauchy elastic anyway) and simulate its stiffness response. The conformal curvature allows then for an insensitive interpolation between these values and the large scale, classical limit, see Figure 4.

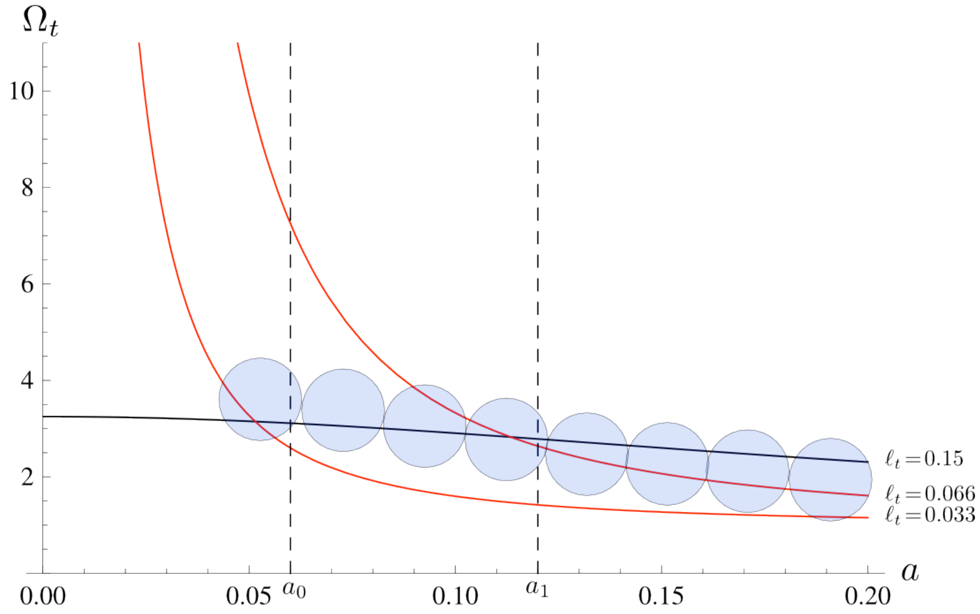

Figure 7: Identification of length scale ℓ_t based on an artificial set of data points (circles). Assume in the first case only data points right to a_1 are considered. Both, the non-singular fit with $\ell_t = 0.15$ and the singular fit with $\ell_t = 0.066$ would give reasonable agreement. If data points to the right of $a_0 = \frac{a_1}{2}$ are considered, then the non-singular fit remains valid while for the singular fit $\ell_t = 0.033$ needs to be taken. Since the last ℓ_t is much smaller than previously the identification of ℓ_t based on the singular response is very sensitive w.r.t. the smallest investigated specimen size. In addition, this example shows that the non-singular case allows for ℓ_t values orders of magnitude larger than in the singular case.

The determination of the four remaining constants proceeds then as follows. The values $(E, \nu) \sim (\mu, \lambda)$ are determined in size-independent classical tension tests. The values $(N, \ell_t) \sim (\mu_c, \ell_t)$ are determined from independent bending and torsion experiments: μ_c is given in a size-independent way from the maximal stiffness increase in torsion observed from the smallest sample (2.9) and ℓ_t is determined by curve-fitting from the same test. The bending test can then be used as a cross-check.

In Figure 7 we see that the genuinely similar curves (same order) for $\boldsymbol{\Omega}_{\mathrm{t}}$ may be fitted by different sets of parameter-values in the singular and non-singular case. In order to arrive at the same approximative value of $\boldsymbol{\Omega}_{\mathrm{t}}$ in the singular case one must choose ℓ_t one order of magnitude smaller as compared to the bounded stiffness case. The approximation depends also on the smallest cut off length in a sensitive way: extending to half the smallest value (with a bounded behaviour) implies to use a much smaller ℓ_t.

If boundary value problems are considered where microrotations remain free at the boundary (for torsion around e_3-axis $m_{33} = 0$ at the top and bottom of the cylinder), then one has yet another mechanism to counter balance the singular response, namely by taking $\mu_c \ll \mu$. This seems to be the deeper reason why usually $\mu_c \ll \mu$ is considered [9, p.166]. Unfortunately, for this case analytical solutions do not seem to exist and one has to resort to finite-element computations [20, 31, 26].

5 Conclusion

Within our restriction on full three-dimensional analytical solutions we obtain from bounded normalised stiffness in torsion and bending the conformal curvature expression. In that case, μ_c is determined as a size-independent quantity. Interestingly, the result does not carry over to the indeterminate couple stress problem. This suggests that the Cosserat model may be more adequate in treating size-effects than the indeterminate couple stress problem in general.

References

[1] E.L. Aero and E.V. Kuvshinskii. Fundamental equations of the theory of elastic media with rotationally interacting particles. *Soviet Physics-Solid State*, 2:1272–1281, 1961.

[2] W.B. Anderson and R.S. Lakes. Size effects due to Cosserat elasticity and surface damage in closed-cell polymethacrylimide foam. *J. Mat. Sci.*, 29:6413–6419, 1994.

[3] A. Anthoine. Effect of couple-stresses on the elastic bending of beams. *Int. J. Solids Struct.*, 37:1003–1018, 1998.

[4] D. Bigoni and W.J. Drugan. Analytical derivation of Cosserat moduli via homogenization of heterogeneous elastic materials. *J. Appl. Mech.*, 74:741–753, 2007.

[5] M. Ciarletta and D. Iesan. *Non-classical elastic solids.* Pitman Research Notes in Mathematics Series. Longman Scientific, Essex, 1993.

[6] E. Cosserat and F. Cosserat. *Théorie des corps déformables.* Librairie Scientifique A. Hermann et Fils (engl. translation by D. Delphenich 2007, pdf available at http://www.mathematik.tu-darmstadt.de/fbereiche/analysis/pde/staff/neff/patrizio/Cosserat.html), Paris, 1909.

[7] S. Cowin. An incorrect inequality in micropolar elasticity theory. *Z. Angew. Math. Physik*, 21:494–497, 1970.

[8] J. Dyszlewicz. *Micropolar Theory of Elasticity.*, volume 15 of *Lecture Notes in Applied and Computational Mechanics.* Springer, Heidelberg, 2004.

[9] A. C. Eringen. *Microcontinuum Field Theories.* Springer, Heidelberg, 1999.

[10] N.A. Fleck, G.M. Müller, M.F. Ashby, and J.W. Hutchinson. Strain gradient plasticity: theory and experiment. *Acta. Metall. Mater.*, 42(2):475–487, 1994.

[11] S. Forest. Cosserat media. In *Encyclopedia of Materials: Science and Technology.*, pages 1715–1718. Elsevier, 2001.

[12] R.D. Gauthier. Experimental investigations on micropolar media. In O. Brulin and R.K.T. Hsieh, editors, *Mechanics of Micropolar Media*, pages 395–463. CISM Lectures, World Scientific, Singapore, 1982.

[13] R.D. Gauthier and W.E. Jahsman. A quest for micropolar constants. *ASME J. Appl. Mech.*, 42:369–374, 1975.

[14] R.D. Gauthier and W.E. Jahsman. Bending of a curved bar of micropolar elastic material. *ASME J. Appl. Mech.*, 43:502–503, 1976.

[15] P. Grammenoudis and C. Tsakmakis. Predictions of microtorsional experiments by micropolar plasticity. *Proc. Roy. Soc. London A*, 461:189–205, 2005.

[16] G. Grioli. Elasticitá asimmetrica. *Ann. Mat. Pura Appl., Ser. IV*, 50:389–417, 1960.

[17] D. Iesan. Bending of a micropolar elastic beam by terminal couples. *Analele Stiintifice Universitatii Iasi Mathematica*, 17:483–490, 1971.

[18] D. Iesan. St.-Venants problem for inhomogeneous and anisotropic Cosserat elastic solids. *Z. Angew. Math. Mech.*, 58:95–99, 1978.

[19] J. Jeong and P. Neff. Existence, uniqueness and stability in linear Cosserat elasticity for weakest curvature conditions. *Preprint 2550, http://www3.mathematik.tu-darmstadt.de/fb/mathe/bibliothek/preprints.html, Math. Mech. Solids, doi:10.1177/1081286508093581*, 2008.

[20] J. Jeong, H. Ramezani, I. Münch, and P. Neff. A numerical study for linear isotropic Cosserat elasticity with conformally invariant curvature. *Preprint 2558, http://www3.mathematik.tu-darmstadt.de/fb/mathe/bibliothek/preprints.html, submitted to Z. Angew. Math. Mech.*, 2009.

[21] W.T. Koiter. Couple stresses in the theory of elasticity I,II. *Proc. Kon. Ned. Akad. Wetenschap*, B 67:17–44, 1964.

[22] R.S. Lakes. Experimental microelasticity of two porous solids. *Int. J. Solids Struct.*, 22:55–63, 1985.

[23] R.S. Lakes. Experimental methods for study of Cosserat elastic solids and other generalized elastic continua. http://silver.neep.wisc.edu/∼lakes/CossRv.pdf. In H.B. Mühlhaus, editor, *Continuum Models for Materials with Microstructure.*, pages 1–25. Wiley, 1995.

[24] R.S. Lakes. On the torsional properties of single osteons. *J. Biomech.*, 25:1409–1410, 1995.

[25] R.D. Mindlin and H.F. Tiersten. Effects of couple stresses in linear elasticity. *Arch. Rat. Mech. Anal.*, 11:415–447, 1962.

[26] I. Münch. *Ein geometrisch und materiell nichtlineares Cosserat-Modell - Theorie, Numerik und Anwendungmöglichkeiten.* Dissertation in der Fakultät für Bauingenieur-, Geo- und Umweltwissenschaften, ISBN 978-3-935322-12-6, electronic version available at http://digbib.ubka.uni-karlsruhe.de/volltexte/1000007371, Karlsruhe, 2007.

[27] P. Neff. The Cosserat couple modulus for continuous solids is zero viz the linearized Cauchy-stress tensor is symmetric. *Preprint 2409, http://www3.mathematik.tu-darmstadt.de/fb/mathe/bibliothek/preprints.html, Z. Angew. Math. Mech.*, 86:892–912, 2006.

[28] P. Neff and J. Jeong. A new paradigm: the linear isotropic Cosserat model with conformally invariant curvature energy. *Preprint 2559, http://www3.mathematik.tu-darmstadt.de/fb/mathe/bibliothek/preprints.html, to appear in Z. Angew. Math. Mech.*, 2009.

[29] P. Neff, J. Jeong, I. Münch, and H. Ramezani. Mean field modeling of isotropic random Cauchy elasticity versus microstretch elasticity. *Preprint 2556, http://www3.mathematik.tu-darmstadt.de/fb/mathe/bibliothek/preprints.html, to appear in Z. Angew. Math. Phys.*, 2009.

[30] P. Neff, J. Jeong, and H. Ramezani. Subgrid interaction and micro-randomness - novel invariance requirements in infinitesimal gradient elasticity. *Preprint 2568, http://www3.mathematik.tu-darmstadt.de/fb/mathe/bibliothek/preprints.html, submitted*, 10/2008.

[31] P. Neff, I. Münch, and W. Wagner. Constitutive parameters for a nonlinear Cosserat model. A numerical study. *Oberwolfach Reports 52/2005, European Mathematical Society*, 2(4):2994, 2005.

[32] S. Nikolov, C.S. Han, and D. Raabe. On the origin of size effects in small-strain elasticity of solid polymers. *Int. J. Solids Struct.*, 44:1582–1592, 2007.

[33] W. Nowacki. *Theory of Asymmetric Elasticity. (polish original 1971)*. Pergamon Press, Oxford, 1986.

[34] V.A. Palmov. Fundamental relations of the theory of asymmetric elasticity theory. *Prikl. Mat. Mekh.*, 28:401–408, 1964.

[35] S. Potapenko, P. Schiavone, and A. Mioduchowski. On the solution of the torsion problem in linear elasticity with microstructure. *Math. Mech. Solids*, 11:181–195, 2006.

[36] G.V. Krishna Reddy and N.K. Venkatasubramanian. On the flexural rigidity of a micropolar elastic circular cylinder. *ASME J. Appl. Mech.*, 45:429–431, 1978.

[37] P. Steinmann. A unifying treatise of variational principles for two types of micropolar continua. *Acta Mech.*, 121:215–232, 1997.

[38] R.A. Toupin. Elastic materials with couple stresses. *Arch. Rat. Mech. Anal.*, 11:385–413, 1962.

[39] F. Yang, A.C.M. Chong, D.C.C. Lam, and P. Tong. Couple stress based strain gradient theory for elasticity. *Int. J. Solids Struct.*, 39:2731–2743, 2002.

[40] J. F. C. Yang and R.S. Lakes. Transient study of couple stress effects in human compact bone. *J. Biomechanical Engineering*, 103:275–279, 1981.

Notation

Let $\Omega \subset \mathbb{R}^3$ be a bounded domain with Lipschitz boundary $\partial\Omega$ and let Γ be a smooth subset of $\partial\Omega$ with non-vanishing 2-dimensional Hausdorff measure. For $a, b \in \mathbb{R}^3$ we let $\langle a, b\rangle_{\mathbb{R}^3}$ denote the scalar product on $\mathbb{R}^3$ with associated vector norm $\|a\|^2_{\mathbb{R}^3} = \langle a, a\rangle_{\mathbb{R}^3}$. We denote by $\mathbb{M}^{3\times3}$ the set of real 3×3 second order tensors, written with capital letters and Sym denotes symmetric second orders tensors. The standard Euclidean scalar product on $\mathbb{M}^{3\times3}$ is given by $\langle X, Y\rangle_{\mathbb{M}^{3\times3}} = \operatorname{tr}\left[XY^T\right]$, and thus the Frobenius tensor norm is $\|X\|^2 = \langle X, X\rangle_{\mathbb{M}^{3\times3}}$. In the following we omit the index $\mathbb{R}^3, \mathbb{M}^{3\times3}$. The identity tensor on $\mathbb{M}^{3\times3}$ will be denoted by $1\!\!1$, so that $\operatorname{tr}[X] = \langle X, 1\!\!1\rangle$. We set $\operatorname{sym}(X) = \frac{1}{2}(X^T + X)$ and $\operatorname{skew}(X) = \frac{1}{2}(X - X^T)$ such that $X = \operatorname{sym}(X) + \operatorname{skew}(X)$. For $X \in \mathbb{M}^{3\times3}$ we set for the deviatoric part $\operatorname{dev} X = X - \frac{1}{3}\operatorname{tr}[X]\, 1\!\!1 \in \mathfrak{sl}(3)$ where $\mathfrak{sl}(3)$ is the Lie-algebra of traceless matrices. The set $\operatorname{Sym}(n)$ denotes all symmetric $n\times n$-matrices. The Lie-algebra of $\mathrm{SO}(3) := \{X \in \mathrm{GL}(3) \mid X^T X = 1\!\!1,\ \det[X] = 1\}$ is given by the set $\mathfrak{so}(3) := \{X \in \mathbb{M}^{3\times3} \mid X^T = -X\}$ of all skew symmetric tensors. The canonical identification of $\mathfrak{so}(3)$ and $\mathbb{R}^3$ is denoted by $\operatorname{axl}\overline{A} \in \mathbb{R}^3$ for $\overline{A} \in \mathfrak{so}(3)$. Note that $(\operatorname{axl}\overline{A}) \times \xi = \overline{A}.\xi$ for all $\xi \in \mathbb{R}^3$, such that

$$\operatorname{axl}\begin{pmatrix} 0 & \alpha & \beta \\ -\alpha & 0 & \gamma \\ -\beta & -\gamma & 0 \end{pmatrix} := \begin{pmatrix} -\gamma \\ \beta \\ -\alpha \end{pmatrix}, \quad \overline{A}_{ij} = \sum_{k=1}^{3} -\varepsilon_{ijk} \cdot \operatorname{axl}\overline{A}_k\,,$$
$$\|\overline{A}\|^2_{\mathbb{M}^{3\times3}} = 2\,\|\operatorname{axl}\overline{A}\|^2_{\mathbb{R}^3}\,, \qquad \langle\overline{A}, \overline{B}\rangle_{\mathbb{M}^{3\times3}} = 2\langle\operatorname{axl}\overline{A}, \operatorname{axl}\overline{B}\rangle_{\mathbb{R}^3}\,, \tag{5.1}$$

where ε_{ijk} is the totally antisymmetric permutation tensor. Here, $\overline{A}.\xi$ denotes the application of the matrix $\overline{A}$ to the vector ξ and $a \times b$ is the usual cross-product. Moreover, the inverse of axl is denoted by anti and defined by

$$\begin{pmatrix} 0 & \alpha & \beta \\ -\alpha & 0 & \gamma \\ -\beta & -\gamma & 0 \end{pmatrix} := \operatorname{anti}\begin{pmatrix} -\gamma \\ \beta \\ -\alpha \end{pmatrix}, \quad \operatorname{axl}(\operatorname{skew}(a \otimes b)) = -\frac{1}{2}\, a \times b\,, \tag{5.2}$$

and

$$2\operatorname{skew}(b \otimes a) = \operatorname{anti}(a \times b) = \operatorname{anti}(\operatorname{anti}(a).b)\,. \tag{5.3}$$

Moreover,

$$\operatorname{curl} u = 2\operatorname{axl}(\operatorname{skew}\nabla u)\,. \tag{5.4}$$